Polymer Chemistry

ROYAL SOCIETY OF CHEMISTRY

PAPER

View Article Online
View Journal | View Issue

Cite this: *Polym. Chem.*, 2026, **17**, 724

Controlled synthesis and post-modification of polypentafluorostyrene in continuous flow

Alexander P. Grimm, [a] Amna B. Asghar, [b] Björn Schmidt, [a] Christian W. Schmitt, [a] Dominik Voll, [c] Tanja Junkers [b] and Patrick Théato *[a,c]

The establishment of automation of laboratory research over the past years has rapidly advanced all fields of chemical science including polymer synthesis. However, automated synthesis of polymers is largely limited to non-functional materials and post-polymerisation modification (PPM) remains underrepresented in flow polymer science. Herein, the polymerisation and PPM of pentafluorostyrene (PFSty), an established precursor polymer for PPM *via para*-fluoro-thiol-reaction (PFTR), in continuous flow is reported for the first time. The kinetic behaviour of the reversible addition–fragmentation chain transfer (RAFT) polymerisation of PFSty *via* transient timesweeping is demonstrated, yielding apparent polymerisation rate coefficients of 1.18×10^{-3} to 1.13×10^{-2} s^{-1} at 70–90 °C with 2-cyano-2-propyldodecyltrithiocarbonate (CPDT) as RAFT agent. Consequently, the PFTR of poly(PFSty) in continuous flow is investigated using 1-dodecanethiol (DT), 4-fluorobenzyl mercaptan (FBM), and 4-trifluoromethylbenzyl mercaptan (TFBM) showing quantitative conversion of FBM and TFBM after 6 min at 60 °C while DT does not exceed 53% modification of poly(PFSty) at 70 °C. Finally, a mixed flow-PFTR concept enables predictable copolymer modification with thiol mixtures through direct syringe pump control, achieving up to 99% precision depending on thiol reactivity. The proposed strategy offers a versatile approach for the continuous-flow synthesis and modification of reactive polymers, expanding the library of functional polymers for high-throughput methodologies.

Received 1st December 2025,
Accepted 9th January 2026

DOI: 10.1039/d5py01142f

rsc.li/polymers

Introduction

In recent years, the utilisation of continuous flow for investigation of chemical syntheses and characterisation has experienced an unprecedented upswing with the establishment of computer-assisted reaction management.[1] Artificial intelligence (AI) and machine learning (ML) have proven effective in accelerating data acquisition, curation, and processing to meet the requirements of modern materials and data scientists.[2] By employing continuous reaction control in a flow reactor setup, rapid feedback on the state of a reaction and the product quality is achieved by virtue of in- and online analysis.[3] Today, the use of AI and ML has entered every field of chemical research from organic[4,5] to inorganic[6,7] chemistry and researchers have acknowledged the potential of these tools for a more precise and time-saving method for experiment design and analysis with less trial-and-error setbacks.[8] Given its environmental and industrial relevance and scope, the field of polymer chemistry is of special interest for the usage of advanced flow techniques. The annual production of plastics and synthetic polymers has been projected to be 1.1 billion tons by the year of 2050 and more efficient material development is therefore imperative for more sustainable chemical research.[9,10] Flow-based polymerisation methods benefit from a number of advantages over conventional batch-based approaches such as the operation under extreme conditions,[11,12] fast mixing of reactants,[13] large surface area for improved heat transfer,[14] increased safety,[15,16] facile scalability,[17] and good reproducibility[18,19] among others which in turn lead to improved overall sustainability.[20] Control over the structure of macromolecules in terms of architecture, molecular weight, and molar mass dispersity ($Đ$) is of utmost importance in order to control material properties and their applications. Among the many established polymerisation techniques, reversible deactivation radical polymerisation (RDRP) and ionic polymerisation methods are used to create polymers with defined architectures, controlled molecular weight and low $Đ$. With anionic polymerisation being historically the first example for continuous flow polymerisations,[21–24] RDRP methods are widely used in flow polymer chemistry research owing to their chemical robustness, versatility, and straightforward execution.[25] RAFT poly-

[a]*Institute for Biological Interfaces III (IBG-3), Karlsruhe Institute of Technology (KIT), Hermann-von-Helmholtz-Platz 1, 76344 Eggenstein-Leopoldshafen, Germany. E-mail: patrick.theato@kit.edu*
[b]*Polymer Reaction Design Group, School of Chemistry, Monash University, 19 Rainforest Walk, Clayton, 3800 Victoria, Australia*
[c]*Institute for Technical Chemistry and Polymer Chemistry (ITCP), Karlsruhe Institute of Technology (KIT), Engesserstr. 18, 76131 Karlsruhe, Germany*

merisation has proven to be especially versatile and useful in a flow chemistry context with recent advancements including photoiniferter-RAFT,[26–28] ultrasound-assisted RAFT,[29,30] polymerisation-induced self-assembly (PISA),[31–33] and depolymerisation.[34,35] One key advantage of chemistry in continuous flow is the ability to acquire and analyse large timed datasets from small reaction volumes through flow manipulation, which has been pioneered by Girkin *et al.* in 2011[36] and Jensen *et al.* in 2013.[37] It was later adopted for polymer chemistry as a method called transient timesweeping (TT).[38] A detailed explanation of TT can be found in a work published by van Herck and Junkers in 2021.[39] In contrast to a self-learning, closed-loop multi objective optimisation,[40–42] TT is a method to obtain kinetic information about a given reaction by analysing the transient reaction volume between two flow rates. Continuous analysis of the monomer conversion (p) during the equilibration period after a change in flow rate from A to B results in a screening through all transient residence times and yields a full kinetic profile between the residence times attributed to flow rates A and B.[39] Inline nuclear magnetic resonance (NMR) spectroscopy and online size exclusion chromatography (SEC) are typically used to monitor p and molecular weight development during the reaction. In recent years, TT has been successfully employed to investigate the polymerisation behaviour of commodity monomers such as numerous acrylates[26,28,43,44] and styrene.[45] However, the investigation of functional monomers in TT experiments remains underrepresented and is believed to be a promising tool to accelerate material development from modifiable platform polymers able to undergo PPM. Poly (pentafluorostyrene) (poly(PFSty)), used for adjustably wettable surfaces,[46] low dielectric films,[47] PISA of nanoparticles,[48] and ionic liquids[49] is known to efficiently undergo PPM *via* PFTR with thiols under presence of bases such as triethylamine or diazabicycloundecene (DBU). The PFTR is highly selective and can be carried out under mild conditions, classifying it as a 'quasi-click' reaction.[50] To the best of our knowledge, PFSty has to this day not been investigated in terms of flow polymerisation behaviour and neither has the PPM of poly(PFSty) in flow. We believe that enabling poly(PFSty) as platform for highly efficient material development through PFTR in continuous flow is a promising approach to advance next-generation automated polymer research.

Herein, we extend our previous study on the automated RAFT polymerisation and modification of pentafluorophenyl acrylate (PFPA) in continuous flow[51] to the kinetic investigation of the polymerisation of PFSty by virtue of TT. Additionally, we report the efficient PPM of poly(PFSty) *via* flow-PFTR which allowed precise control over polymer structures and material properties.

Experimental

Materials

1,8-Diazabicyclo(5.4.0)undec-7-ene (DBU) (Alfa Aesar, 99%), 1-dodecanethiol (DT) (Sigma Aldrich, ≥98%), 2-(dodecylthiocarbonothioylthio)propionic acid (CDCTPA) (Boron Molecular, 97%), 2,3,4,5,6-pentafluorostyrene (PFSty) (BLD Pharmatech, 98%), 2-cyano-2-propyldodecyltrithiocarbonate (CPDT) (BLD Pharmatech, 97%), 2-cyanobutan-2-yl 4-chloro-3,5-dimethyl-1*H*-pyrazole-1-carbodithioate (CBCDMPC) (Boron Molecular, 95%), 4-fluorobenzyl mercaptan (FBM) (BLD Pharmatech, 98%), 4-trifluoromethylbenzyl mercaptan (TFBM) (BLD Pharmatech, 95%), dimethylformamide (DMF) (Thermo Scientific, 99.8% over molecular sieve), methanol (Carl Roth, technical grade), petrol ether (PE) (Carl Roth, technical grade), and tetrahydrofuran (THF) (Acros Organics, 99.8%) were used as received. Azobisisobutyronitrile (AIBN) (Sigma-Aldrich, 98%) was recrystallised from methanol prior to use. 4-Cyano-4-[[(dodecylthio) carbonothioyl]thio] pentanoic acid (DoPAT) was synthesised according to literature.[52]

Characterisation

Differential scanning calorimetry (DSC) was performed on a 214 Polyma DSC device from NETZSCH (Selb, Germany). Around 5 mg of sample were precisely (Δ = 0.005 mg) weighed in an aluminium pan with a pierced lid for measurement. An aluminium pan filled with air was used as a reference and the heating rate was typically set to 10 K min^{-1} for all measurements. Only the second heating run was used for discussion unless stated otherwise.

High-field NMR spectra were recorded using an Ascend 400 MHz spectrometer from Bruker (Billerica, Massachusetts, USA). Samples were dissolved in deuterated solvents, and the number of scans was typically set to 256 unless stated otherwise. Low-field NMR spectra were recorded on a 60 MHz Spinsolve 60 Ultra from Magritek (Aachen, Germany) (acquisition bandwidth 5 kHz: 83 ppm; acquisition time: 6.554 seconds; relaxation time: 17 seconds).

SEC measurements of isolated polymer samples were conducted using a Tosoh EcoSEC (Tokyo, Japan) SEC system equipped with a SDV 5 μm bead size guard column (50 × 8 mm) followed by three SDV 5 μm columns (300 × 7.5 mm, subsequently 100, 1000, and 105 Å pore size). THF was used as eluent at 35 °C with a flow rate of 1.0 mL min^{-1}. The SEC system was calibrated by using linear polystyrene standards with the Mark–Houwink-parameters K = 0.01363 mL g^{-1} and α = 0.714. Online SEC was performed on a custom-designed PSS system, operated by PSS WinGPC software. The SEC was equipped with a PSS SDV analytic column (50 × 8 mm), followed by one PSS SDV analytic 3.0 μm particle with porosity of 1000 Å (300 × 8 mm). The sample was analyzed *via* an evaporative light scattering detector (ELSD) ELS1300 using THF as eluent at 40 °C with a flow rate of 1 mL min^{-1}. The SEC system was calibrated with linear narrow polystyrene standards ranging from 474 to 7.5 × 10^6 g mol^{-1} (K = 1.41 × 10^{-4} dL g^{-1} and α = 0.70). Due to the inherent inaccuracy of SEC for materials that differ from the calibration polymer, molecular weights were rounded to the second digit.[53]

Thermogravimetric analysis (TGA) was conducted using a TGA 5500 from TA Instruments (Eschborn, Germany) in Platinum HT pans under nitrogen atmosphere. Samples were

equilibrated at 30 °C and heated to 800 °C at a heating rate of 10 K min^{-1}. 5–10 mg of sample were used per measurement.

Synthesis of DoPAT

In a 500 mL round bottom flask, 2.28 g NaOH (57.05 mmol, 1.00 eq.) and 1.22 g tetrapropylammonium bromide (4.56 mmol, 0.08 eq.) were dissolved in a mixture of 11.55 g 1-dodecanethiol (57.05 mmol, 1.00 eq.) with 200 mL acetone and 25 mL DI water. 4.34 g CS_2 (57.05 mmol, 1.00 eq.) were added, and the reaction solution was stirred for 30 min at ambient temperature (a.t.). 8.73 g 2-bromopropionic acid (57.05 mmol, 1.00 eq.) were added and the reaction mixture was stirred for further 18 h at a.t. The acetone was removed under reduced pressure, and the resulting solution was acidified with 100 mL 1 M HCl solution and diluted with 100 mL DI water. The precipitate was collected *via* glass filter and recrystallised once from petrol ether at a.t. Drying overnight under vacuum gave DoPAT in the form of a yellow solid (yield: 78%).

Transient timesweeping of PFSty in continuous flow

The flow setup used for the polymerisation of PFSty followed a previously described setup used for polymerization of methyl acrylate (MA) and methyl methacrylate (MMA).[28] In brief, 7.50 g PFSty (38.64 mmol), 267 mg CPDT (0.773 mmol), and 25 mg AIBN (0.155 mmol) were dissolved in 18.5 mL anhydrous DMF. The solution was degassed with argon for 10 minutes before the solution was transferred to a 50 mL gastight syringe from SGE which was placed in a Chemyx syringe pump. The tubular reactor comprised of a PFA tubing with a volume of 2 mL, submerged in a preheated oil bath with constant temperature. Monomer conversion was continuously recorded by a 60 MHz benchtop NMR, and the flow rate and SEC injections were controlled by a custom python script (for table with flow rates for each respective timesweep, refer to SI, Table S1).

Kinetic post-polymerisation modification study of poly(PFSty) in continuous flow *via* flow-PFTR

The flow setup for the kinetic investigation of the PFTR of poly (PFSty) in continuous flow consisted of three syringe pumps connected to a heated flow reactor with a volume of 1 mL. 1.50 g of poly(PFSty) (7.73 mmol of reactive units) were dissolved in 30 mL anhydrous DMAc, and the solution was loaded into syringe 1. 7.73 mmol of the respective thiol and 1.12 g of DBU (7.73 mmol) were dissolved in 15 mL anhydrous DMAc. The solutions were loaded in syringes 2 and 3, respectively. The streams of syringes 2 and 3 were merged, before combining with the stream of syringe 1. The flow rates were adjusted to result in residence times of 1, 2, 3, 6, 9, 12, and 15 minutes in the reactor (for table with flow rates for each respective sample, refer to SI, Table S2). The kinetic screening was conducted at 50, 60, and 70 °C. The polymers were isolated by direct precipitation in cold PE after exiting the reactor, followed by centrifugation and drying in vacuum at 40 °C for 18 h.

Post-polymerisation modification of poly(PFSty) in continuous flow *via* mixed flow-PFTR

The flow setup used for the PPM of poly(PFSty) was based on our previously described setup for the PPM of poly(pentafluorophenyl acrylate)[51] and has been extended with another syringe pump. In brief, 2.00 g of poly(PFSty) (10.30 mmol of reactive units) were dissolved in 20 mL anhydrous DMAc and the solution was loaded in syringe 1. 10.30 mmol of DT or FBM and 10.30 mmol of FBM or TFBM were dissolved in 10 mL anhydrous DMAc and loaded into syringes 2 and 3, respectively and depending on the desired thiol mixtures. 3.14 g DBU (20.60 mmol) were dissolved in 20 mL anhydrous DMAc, and the solution was loaded to syringe 4. The 3D-printed metal flow reactor was heated to the desired temperature and dosing of the syringe pumps started. After each flow rate change, a total of 2 mL was passed through the system before 2 mL samples were collected (for table with flow rates for each respective sample, refer to SI, Table S3). The polymers were isolated by direct precipitation in cold PE after exiting the reactor, followed by centrifugation and drying in vacuum at 40 °C for 18 h.

Results and discussion

Polymerisation of PFSty

TT experiments of the RAFT polymerisation of PFSty were conducted using different RAFT agents in order to evaluate their suitability and polymerisation performance in terms of monomer conversion, molar mass distribution, and control over the reaction (refer to Fig. 1A; for more details on the reaction platform, refer to SI).[54] In a standard TT experiment, a DMF solution containing PFSty, a RAFT agent, and AIBN was prepared at molar ratios of 50 : 1 : 0.2, respectively. For each run, PFSty accounted for 30 wt% of the total reaction mixture (refer to Fig. 1B). CPDT, CDCTPA, DoPAT, and CBCDMPC were chosen as RAFT agents (refer to Fig. 1C). For practicability purposes, the maximum reaction time was set to 60 min and was separated into 4 timesweeps: 4–8 min, 8–16 min, 16–32 min, and 32–60 min to prevent "smearing" due to sudden changes in back pressure and exit of the analyte from the NMR-sensitive volume before all spins have relaxed.[39] Monomer conversion was quantified by ^{1}H NMR spectroscopy using the standard Magritek flow reaction monitoring protocol, acquiring one scan every 17 s throughout the experiment. Data from stabilisation and waiting periods were excluded, and the remaining timesweeps were combined into a single conversion–residence time profile. Conversion was calculated from the ratio of C=C double-bond proton signals to the constant DMF formamide proton signal (H–C=O), using the known initial ratio prior to reaction. SEC measurements were performed by continuous sample injection following a delay to account for the dead volume between the reactor and the injection valve. During passage of the transient volume, SEC runs were initiated every 180 s at the new equilibrium flow rate. The number and density of SEC measurements within a transient

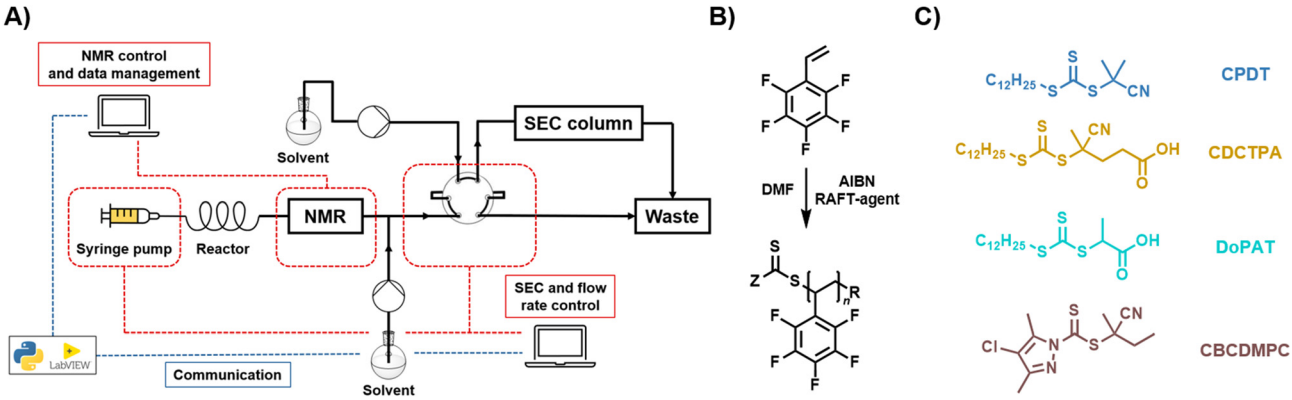

Fig. 1 (A) Schematic setup used for the high-throughput investigation of the polymerisation of PFSty *via* TT. Dashed red lines indicate hardware control between computer and devices. Dashed blue lines indicate software communication between computers. (B) Reaction scheme of the RAFT polymerisation of PFSty in DMF with AIBN. (C) Chemical structures of the RAFT agents investigated in this study.

volume depended on the flow rate and timesweep duration. For example, a 4–8 min timesweep yielded four SEC traces (4, 5.5, 7, and 8 min residence times), whereas an 8–16 min timesweep produced seven traces (8, 9.5, 11, 12.5, 14, 15.5, and 16 min). TT experiments with CPDT, CDCTPA, DoPAT, and CBCDMPC as RAFT agents at 85 °C showed a mostly linear increase in monomer conversion with residence time (refer to Fig. 2A). DoPAT-mediated polymerisation exhibited the highest propagation rate, achieving 49.0% monomer conversion after 60 min residence time. Assuming pseudo-first-order kinetics, the apparent polymerisation rate coefficient can be calculated from the slope of the linear regression of the natural logarithm of conversion *versus* time (refer to SI, Table S4). However, SEC analysis showed the incompatibility of DoPAT with PFSty compared to the other investigated RAFT agents, because poly(PFSty) synthesized with DoPAT exhibited a molecular weight of 4700 g mol^{-1} after 4 min residence time, increasing only slightly to 5800 g mol^{-1} at 60 min (refer to Fig. 2B). $Đ$ remained comparatively high (above 1.20) throughout, indicating that the singular *alpha*-methyl group of DoPAT did not sufficiently stabilise the leaving group radical in the RAFT pre-equilibrium (refer to SI, Fig. S2). The rapid M_n increase is attributed to direct PFSty polymerisation by AIBN, effectively bypassing DoPAT as controlling agent, which leads to so-called hybrid polymerisation behaviour, visible as a jump of the degree of polymerisation to a certain level before the main equilibrium takes hold of the reaction.[55] In contrast, CDCTPA and CBCDMPC produced comparable SEC results with low dispersity and near-linear M_n-residence time profiles but achieved lower monomer conversions, making them less efficient than CPDT. The M_n-conversion profile confirmed CPDT as the most effective RAFT agent, delivering the highest conversion and lowest $Đ$ at 85 °C, whereas DoPAT failed to maintain controlled polymerisation (refer to Fig. 2C). Consequently, to assess the control and kinetics of PFSty polymerisation at different temperatures, TT experiments were performed between 70 and 100 °C using CPDT as the RAFT agent. At 70 °C, PFSty polymerisation yielded a conversion below 10% after 1 h residence time, making this temperature unsuitable under the given conditions. The linear fit at 70 °C also showed poor agreement

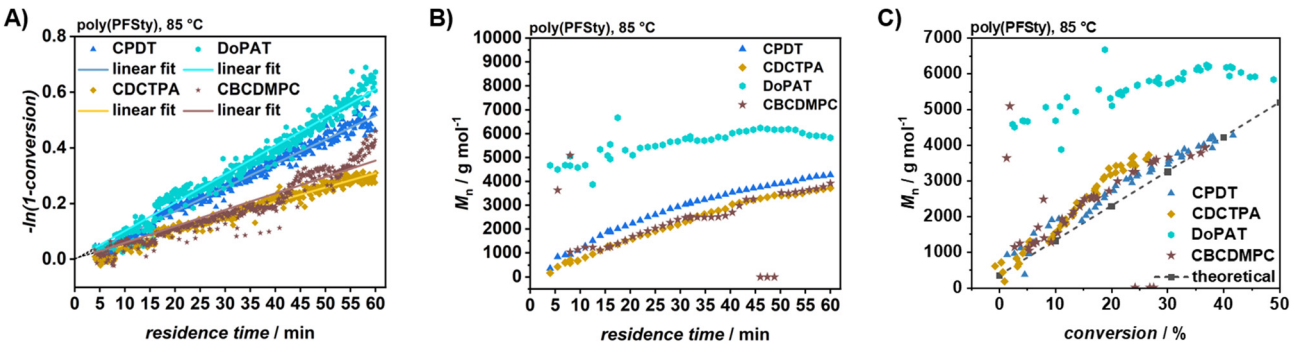

Fig. 2 (A) Pseudo-first-order kinetic plots of poly(PFSty) from four individual timesweeps using different RAFT agents at 85 °C with linear fits. (B) Progression of M_n with increasing residence time using different RAFT agents. (C) M_n *vs.* conversion for the polymerisation of PFSty using different RAFT agents. DoPAT was found to not control the polymerisation of PFSty, rendering it unsuitable for this reaction. Experiments with CPDT, CDCTPA, and CBCDMPC showed good agreement with the theoretical linear increase of M_n with conversion associated with controlled polymerisations.

with experimental data proven by a low R^2 linear fit coefficient of 0.892.

At 100 °C, a nonlinear conversion-time relationship was observed using CPDT as RAFT agent, likely due to increased termination events and a shift toward free-radical polymerisation.[56] In contrast, polymerisation at 80–90 °C was well controlled, achieving satisfactory conversions within 60 min and showing good agreement with linear fits (refer to Fig. 3A and Table 1). The apparent overall polymerisation rate coefficient increased with temperature, consistent with the Arrhenius equation. However, k_{app} at 80 °C was lower than predicted, likely due to experimental preparation errors or NMR shimming inaccuracies during extended operation (refer to SI, Fig. S3). Nonetheless, these results demonstrate the utility of TT as a rapid method for obtaining valuable kinetic data in the synthesis of functional polymers. Monomer conversion could not be determined by ^{19}F NMR due to insufficient signal-to-noise ratio for resolving monomer and polymer signals. Overcoming this would require lower flow rates and increased scan numbers, which, however, contradicts the concept of TT in its essence by disrupting the flow continuity (refer to SI, Fig. S4). Automated SEC acquisition during continuous poly(PFSty) polymerisation enabled monitoring of molecular weight and $Đ$ over time (refer to Fig. 3B and SI, Fig. S5). At 70 °C and 80 °C, M_n of poly(PFSty) increased linearly over time. Raising the temperature to 85–90 °C accelerated chain growth, consistent with the higher k_{app}, though the M_n profile displayed slight curvature, suggesting radical and chain depletion. At 100 °C, M_n plateaued after 30 min, attributed to initiator consumption and chain termination, in agreement with the ^{1}H NMR conversion profile. Dispersity remained below 1.20 across all conditions, confirming good compatibility of CPDT with PFSty. At temperatures of 90 °C and below, $Đ$ values as low as 1.05 were achieved, indicating excellent control (refer to SI, Fig. S6). M_n-conversion plots further confirmed this control, showing linear correlations up to 90 °C, as expected for controlled polymerisations (refer to Fig. 3C).[57] We hypothesise that variation or continuous dosage initiator might be a promising strategy to achieve high a high degree of control over the polymerisation of PFSty in continuous flow to further strengthen its use as platform polymer for PPM. These findings demonstrate the feasibility of high-throughput PFSty RAFT polymerisation with controlled polymer architecture for PPM applications and confirm the reliability of kinetic data obtained *via* TT.

Table 1 Conversion after 60 minutes residence time, apparent polymerisation rate coefficient, and quality of the linear fit at different polymerisation temperatures

Temperature/ °C	p after 60 min/%	k_{app}/s^{-1}	Coefficient of determination R^2
70	7.2	$1.18 \times 10^{-3} \pm 2.01 \times 10^{-5}$	0.892
80	20.6	$3.89 \times 10^{-3} \pm 2.27 \times 10^{-5}$	0.986
85	41.7	$8.61 \times 10^{-3} \pm 2.71 \times 10^{-5}$	0.996
90	47.7	$1.13 \times 10^{-2} \pm 4.40 \times 10^{-5}$	0.994
100	33.7	—	—

Post-polymerisation modification of poly(PFSty) Flow-PFTR

In addition to the kinetic investigation of the polymerisation of PFSty, the PPM of the obtained poly(PFSty) *via* PFTR has been studied to showcase the versatility of flow chemistry for fast reaction iteration and data acquisition at changing reaction conditions. However, conducting the PFTR of as-obtained poly(PFSty) in the presence of DBU yielded polymers with bimodal molecular weight distribution with the second peak occurring at approximately double the molecular weight of the first one. We hypothesise that polymeric dimerisation occurred under cleavage of the RAFT end group and disulfide formation under presence of air and moisture (refer to SI, Fig. S7 and Scheme S1A).[58] Consequently, the RAFT end group was transformed into a non-reactive end group by radical end group transfer with a mixture of AIBN and lauroyl peroxide (LPO) according to literature (refer to SI, Scheme S2B).[59] The successful cleavage of the dodecyl trithiocarbonate end group was confirmed by ^{1}H NMR spectroscopy with the disappearance of

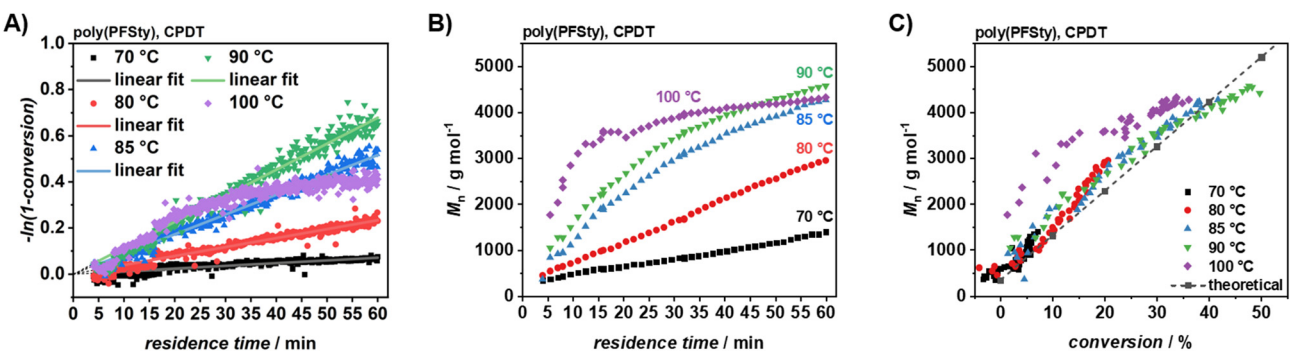

Fig. 3 (A) Pseudo-first-order kinetics plot of poly(PFSty) from four individual timesweeps at different polymerisation temperatures with linear fits. (B) Progression of M_n with increasing residence time. A slight curvature of the *M*n profile appeared at 85 °C and propagation quickly stops at 100 °C. (C) M_n *vs.* conversion for the polymerisation of PFSty at temperatures between 70 and 100 °C. Experiments below 100 °C show good agreement with the theoretical linear increase of *M*n with conversion associated with controlled polymerisations.

the resonances attributed to the CH_2 group adjacent to the trithiocarbonate sulfur at 3.68 ppm (refer to SI, Fig. S8). After removal of the RAFT end group, the kinetic behaviour of the flow-PFTR of poly(PFSty) with 1-dodecanethiol (DT, thiol A), 4-fluorobenzyl mercaptan (FBM, thiol B), and 4-trifluoromethylbenzyl mercaptan (TFBM, thiol C) in presence of DBU in DMAc was investigated and evaluated regarding the reaction conversion. Details on the experimental procedure and the reactor setup can be found in the SI. In short, three syringe pumps with solutions of poly(PFSty), a thiol, and DBU were prepared respectively and connected to a custom-made, temperature-controlled, 3D-printed steel flow reactor. The flow rates of all components were adjusted to result in reactor residence times of 1, 2, 3, 6, 9, 12, and 15 min. Kinetic investigations of the flow-PFTR were conducted at 50, 60, and 70 °C. The PFSty polymers modified *via* flow-PFTR were named poly(PFSty-DT), poly(PFSty-FBM), and poly(PFSty-TFBM), depending on the respective thiol used. For poly(PFSty-DT), the integral ratios between the *para* fluorine atoms of poly(PFSty) and the *meta* fluorine atoms of poly(PFSty-DT) were used to determine the reaction conversion. In poly(PFSty-FBM) and poly(PFSty-TFBM) the reaction conversion was calculated from the integral ratios between the *para* fluorine atom of poly(PFSty) and the aromatic *para* fluorine atom of FBM and the aliphatic CF_3 group of TFBM, respectively (refer to SI, Fig. S9–S11). The flow-PFTR of poly(PFSty) with DT at 50 °C converged after one minute of residence time at a maximum conversion of 45%. While the conversion could be increased to 50% at 60 °C and 53% at 70 °C, it became evident that a longer residence time did not result in higher degree of modification, and the reaction was complete after only one minute (refer to Fig. 4A). The conversion of close to 50% implies the substitution of, on average, every second PFSty unit in the polymer and is believed to be caused by the steric hindrance of DT, which can be overcome, to some extent, by higher reaction temperatures rather than longer reaction times.[60,61] SEC analysis revealed an increase of M_n from 11 400 g mol^{-1} to approximately 17 400 g mol^{-1}. This resembles an increase in M_n with a factor of 1.513 and is close to the expected factor of 1.470 at 50% conversion. The molecular weight distributions were found to remain mono modal and very narrow at $Đ$ = 1.1 before and after the flow-PFTR of poly(PFSty) with DT regardless of the reaction temperature or time (refer to SI, Fig. S12). All SEC measurements in this work were evaluated using polystyrene standards and are intended to identify trends rather than precise values. The flow-PFTR of poly(PFSty) with FBM was found to be very efficient with quantitative conversion after 6 min at 50 °C and 3 min at 70 °C (refer to Fig. 4B). Furthermore, at full conversion, the determined M_n of poly(PFSty-FBM) of approximately 18 200 g mol^{-1} matched the theoretically calculated value of 18 700 g mol^{-1} very closely. However, it was found that $Đ$ increased significantly from 1.1 to 1.26 at longer reaction times and higher temperatures. Thus, residence time and reaction temperature of the flow-PFTR of poly(PFSty) with FBM should ideally not exceed 6 min at 60 °C (refer to SI, Fig. S13). The flow-PFTR of poly(PFSty) with TFBM was found to be significantly slower with full conversions reached after 12 min at 50 °C or 6 min at 60 and 70 °C (refer to Fig. 4C). This can be explained by the reduced nucleophilicity of the TFBM anion compared to the FBM anion due to the strong electron withdrawing CF_3 group. Additionally, TFBM is more sterically demanding than FBM which also affects its reactivity in a nucleophilic substitution.[62] At full conversion, M_n increased from 11 500 g mol^{-1} to 23 000 g mol^{-1} which resembles an increase of factor 2, which is slightly higher than the theoretically expected increase by a factor of 1.88 at full conversion. However, considering the error of SEC measurements, this still confirmed the successful PFTR of poly(PFSty) with TFBM. $Đ$ increased slightly from 1.1 to approximately 1.12 during the reaction (refer to SI, Fig. S14). In summary, the continuous flow approach was shown to be an effective tool to investigate the kinetic behaviour of PPM of poly(PFSty) by flow-PFTR. The flow-PFTR of poly(PFSty) was found to be very efficient at mild conditions with aromatic benzyl thiols as indicated by full conversion at 60 °C after 6 min. In contrast, aliphatic DT was found to undergo PFTR more quickly, but the possible degree of modification was limited to approximately 50%, depending on temperature rather than residence time.

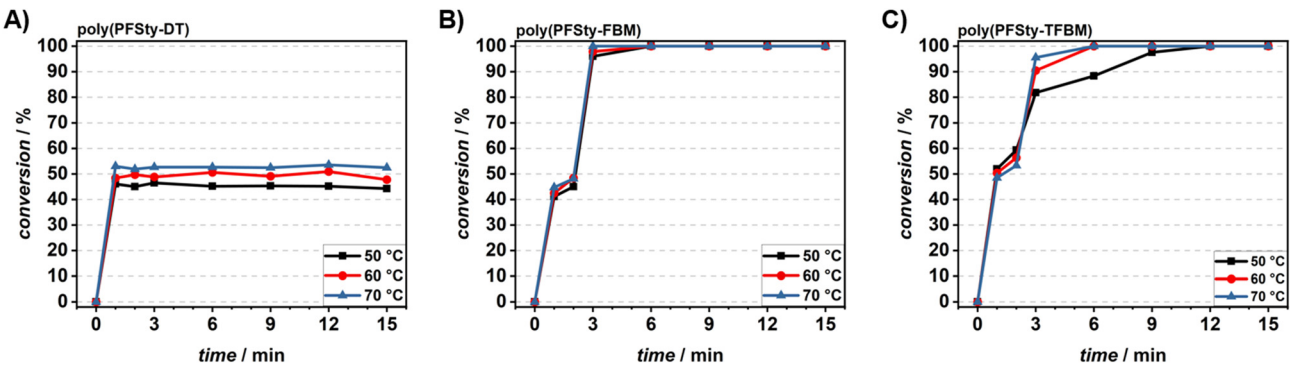

Fig. 4 Conversion-residence time plots of the PFTR of poly(PFSty) with DT (A), FBM (B), and TFBM (C) conducted in continuous flow at 50 °C (black), 60 °C (red), and 70 °C (blue) with DBU as base.

Mixed flow-PFTR – general considerations

Given the versatile modifiability of poly(PFSty) *via* flow-PFTR, a flow reactor setup for precise control over PPM ratios in continuous flow was designed whose setup was published in an earlier work.[51] Building on this study, the flow-PFTR with mixtures of different thiols at changing molar ratios was conducted in order to showcase the versatility of the presented strategy to precisely control molecular compositions of polymer by virtue of flow chemistry to which we will refer to as "mixed flow-PFTR" throughout this article. In general, the PPM flow setup comprised four syringe pumps with syringe 1 containing a solution of poly(PFSty), syringes 2 and 3 contained solutions of two different thiols, and syringe 4 contained a solution of DBU (refer to Fig. 5). The concentrations of thiols and DBU in all solutions were adjusted to match the concentration of active *para* fluorine groups in the polymer solution at any given flow rate combination of the experiment. During the modification experiments, the streams from syringes 2 and 3 were first combined and then merged with the DBU solution from syringe 4. The flow rates of streams 2 and 3 were set so that their combined rate equalled that of the DBU stream and their combined stream in turn equalled that of the polymer solution. The resulting stream contained 10–90 mol% of thiol A and 90–10 mol% of thiol B, respectively, with increments of 10 mol% (A_{10-90}–B_{90-10}). As a result, the total flow rate after mixing of all streams was 0.2 mL min^{-1} for all reaction compositions (refer to SI, Fig. S15). The heated 3D-printed flow reactor had a volume of 1.0 mL, giving a residence time of 5 min. It needs to be noted that a telescoped reaction, where polymerisation and PPM are done in one continuous stream, was not feasible for this study due to expected side reactions. These include reinitiation of polymerisation, thiol–ene reaction, and PFTR with unreacted monomer which were believed to disturb calculation of monomer conversion on one hand and the stochiometric modification of only the polymer on the other. The investigated thiol pairs were DT-FBM, DT-TFBM, and FBM-TFBM and the resulting polymers were named poly(PFSty-DT-*r*-FBM), poly(PFSty-DT-*r*-TFBM), and poly(PFSty-FBM-*r*-TFBM) respectively, where "*r*" indicates the random substitution pattern along the polymer chain. For poly(PFSty-DT-*r*-FBM) and poly(PFSty-DT-*r*-TFBM), the resulting modification ratios between DT and FBM/TFBM were calculated from the ^{1}H NMR integrals attributed to the three terminal CH_3 protons of DT at 0.88 ppm, and the four aromatic FBM/TFBM protons at 6.50–7.50 ppm. Comparison of the found modification ratio in the polymer with the input thiol ratio allowed definition of the precision with which poly(PFSty) could be modified by direct flow rate control of thiols. Interestingly, ^{19}F NMR revealed quantitative conversion of *para* fluorine atoms of poly(PFSty) in all poly(PFSty-DT-*r*-FBM) and poly(PFSty-DT-*r*-TFBM) compositions (refer to SI, Fig. S16). This was unexpected since the flow-PFTR of poly(PFSty) with only DT at 60 °C converged at around 50% conversion (refer to Fig. 4A). A likely explanation for the observed difference in conversion is that the presence of FBM alters both the microenvironment and the reactivity within the polymer matrix. FBM is believed to form a more reactive thiolate with DBU and simultaneously enhances polymer swelling and solvation through π–π and polar interactions with the poly(PFSty) backbone.[63,64] This improved accessibility of reactive sites might enable complete substitution of *para*-fluorine atoms, overcoming the diffusion and steric limitations that restrict conversion to approximately 50% when using DT alone.

Mixed-flow PFTR with DT and FBM

The mixed flow-PFTR of poly(PFSty) with DT and FBM had a very high precision of 88 to 99% throughout the modification range (refer to SI, Fig. S17). It needs to be noted, that the quantitative integration of the DT CH_3 signal might be subject to error due to a slight overlap with competing chemical resonances at low chemical shifts. Additionally, selective reactivity and post-substitution exchange of thioethers may cause devi-

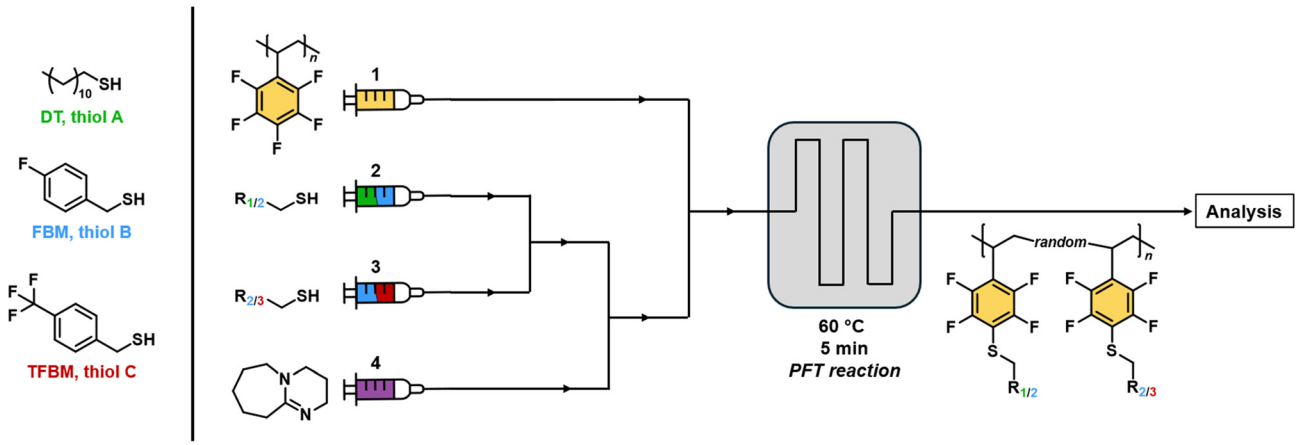

Fig. 5 Chemical structures of DT (green), FBM (blue) and TFBM (red) used in this work (left). Visualisation of the stream connections and the flow reactor setup used for the mixed flow-PFTR of poly(PFSty) at 60 °C. The mixed flow-PFTR was conducted with the following thiol mixtures: DT-FBM, DT-TFBM, and FBM-TFBM with varying thiol ratios for each mixture.

ation of the final modification ratio from the feed ratio.[65,66] Nevertheless, mixed flow-PFTR with DT and FBM yielded very high precision over the modification of poly(PFSty). M_n increased from 19 000 g mol^{-1} to approximately 31 000 g mol^{-1} during the mixed flow-PFTR with DT and FBM, while $Đ$ slightly increased from 1.11 to 1.14–1.15. Interestingly, the trend in M_n matched the expected trend with higher M_n at higher incorporation ratio of the slightly higher molecular weight of DT over FBM, further confirming the tunability of the product polymer by mixed flow-PFTR (refer to SI, Fig. S18). DSC measurements of the polymers showed that the T_g of poly (PFSty) dropped from 88 °C to 62–65 °C after the mixed flow-PFTR, which was overall unaffected by the modification ratio between DT and FBM (refer to SI, Fig. S19). This can be explained by the disruption of PFSty orientation in the material due to the replacement of the *para* fluorine atom by larger substituents which leads to more mobile chains and thus lowers the T_g.[67] Poly(PFSty-DT-*r*-FBM) showed a multistep thermal decomposition profile up to 800 °C with residues of 23 to 39 wt% depending on the modification ratio. It was found that poly(PFSty) is thermally stable up to 381 °C while poly(PFSty-DT-*r*-FBM) started to significantly decompose at temperatures as low as 302 °C (refer to SI, Fig. S20 and Table S5).

Table 2 T_g, $T_{5\%}$, and residual weight at 800 °C of poly(PFSty), poly (PFSty-DT-*r*-FBM), and poly(PFSty-DT-*r*-TFBM). For detailed information, refer to SI

Polymer	T_g/°C	$T_{5\%}$/°C	Weight at 800 °C/wt%
Poly(PFSty)	88	381	0
Poly(PFSty-DT-r-FBM)	62–65	302–315	23–39
poly(PFSty-DT-r-TFBM)	63–65	211–282	27–36

Mixed-flow PFTR with DT and TFBM

Additionally, the mixed flow-PFTR of poly(PFSty) with DT and TFBM was conducted in order to elucidate the structural influence of the CF_3 group of TFBM on the resulting polymers in contrast to the *para* fluorine atom of FBM. The precision of 82–97% was comparable with that of the mixed flow-FPTR with DT and FBM (88–99%). The slightly less precise incorporation of both thiols is most likely caused by the reduced thiolate reactivity of TFBM compared to FBM and the difference in polarity, potentially resulting in local inhomogeneities and occurrence of exchange reactions.[64,66] Nevertheless, mixed flow-PFTR of poly(PFSty) showed satisfactory precision of modification with structurally different thiols (refer to SI, Fig. S21). SEC revealed an increase in M_n from 19 000 g mol^{-1} to approximately 32 200 g mol^{-1} and a slight increase in $Đ$ from 1.11 to 1.14–1.21. However, no clear trend in M_n or $Đ$ could be observed depending on the ratio of modification during the mixed flow-PFTR with DT and TFBM (refer to SI,

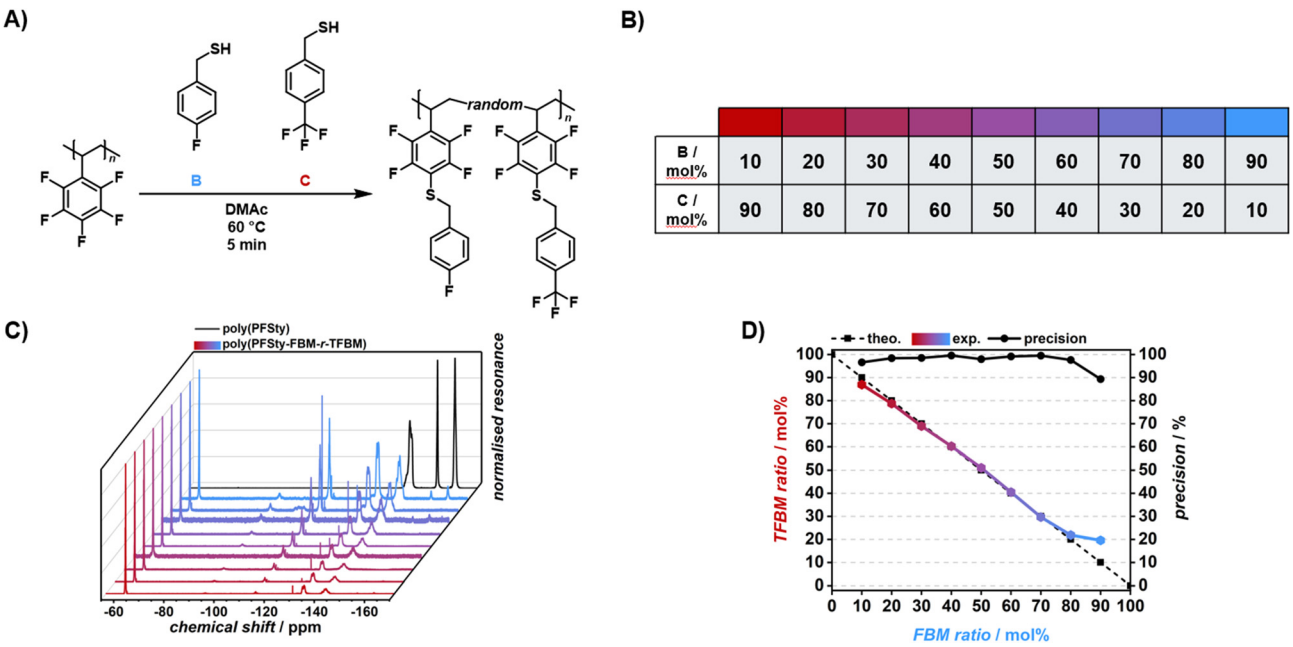

Fig. 6 Reaction scheme of the mixed flow-PFTR of poly(PFSty) with FBM (blue) and TFBM (red) in DMAc at 60 °C. (B) Colour-code for the modification of poly(PFSty) with 10–90 mol% FBM and 90–10 mol% TFBM, respectively. (C) Normalized ^{19}F NMR spectra of poly(PFSty-FBM-*r*-TFBM) in the region between −50 and −150 ppm. The left peak at around −63 ppm is attributed to the aliphatic CF_3 group of TFBM while the peak at around −115 ppm is attributed to the aromatic *para* fluorine atom of FBM. The conversion of *para* fluorine atoms at FBM_{90}-$TFBM_{10}$ was 93%. (D) Theoretical and experimental modification ratios of poly(PFSty) with FBM and TFBM, respectively. The black dashed line represents the theoretical input ratios of FBM and TFBM which are directly linked to the flow rates of the syringe pumps while coloured solid line represents the found ratios in the final polymers. The precision (black circles) describes the deviation of the dashed and the coloured line and shows that excellent control over the modification was obtained.

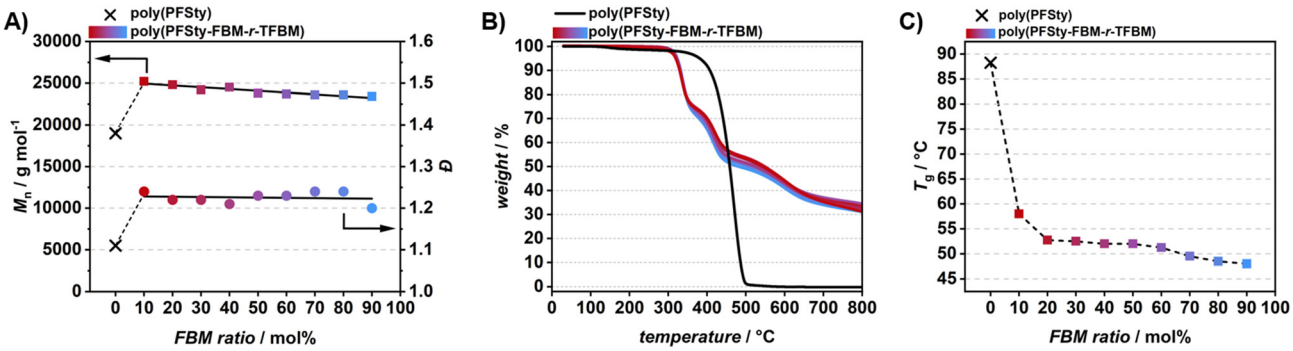

Fig. 7 (A) M_n and $Đ$ of poly(PFSty) (X) and poly(PFSty-FBM-*r*-TFBM) (coloured) at varying thiol ratios. (B) Thermal decomposition of poly(PFSty) and poly(PFSty-FBM-*r*-TFBM) up to 800 °C. Heating rate: 10 K min^{-1}. (C) T_gs of poly(PFSty) (X) and poly(PFSty-FBM-*r*-TFBM) (coloured). Heating rate: 10 K min^{-1}. The amount of FBM increased from red to blue, while the amount of TFBM increased from blue to red, respectively.

Fig. S22). Similar to poly(PFSty-DT-*r*-FBM), poly(PFSty-DT-*r*-TFBM) exhibited a T_g of 64 °C which was independent from the ratio of modification between DT and TFBM which can be explained by the structural similarity between FBM and TFBM (refer to SI, Fig. S23). TGA of poly(PFSty-DT-*r*-TFBM) revealed a thermal decomposition profile with only one distinct decomposition at around 340 °C. While $T_{5\%}$ showed no clear trend depending on the modification ratio, the residual weight at 800 °C decreased linearly with higher amounts of TFBM in the polymer caused by the thermal stability of fluorinated alkyl groups (refer to SI, Fig. S24 and Table S6).[68] For overview, the thermal characteristics of poly(PFSty-DT-*r*-FBM) and poly(PFSty-DT-*r*-TFBM) are summarised in Table 2.

In summary, mixed flow-PFTR using mixtures of aliphatic DT and aromatic FBM/TFBM allowed rapid modification of poly(PFSty) at low temperatures with only 5 min of residence time.

Mixed-flow PFTR with FBM and TFBM

Consequently, the mixed flow-PFTR of poly(PFSty) with FBM and TFBM was conducted, in order to demonstrate the achievable control over the structural modification of poly(PFSty) (refer to Fig. 6A and B). Since both FBM and TFBM contain fluorine atoms, the modification ratio can be directly determined from the integral ratios between the *para* fluorine atom of FBM (at −115 ppm) and the CF_3 atoms of TFBM (at −63 ppm) using ^{19}F NMR spectroscopy (refer to Fig. 6C). In contrast to DT containing mixed flow-PFTR, the precision of modification was excellent with at least 97% in the range of FBM_{10}-$TFBM_{90}$ to FBM_{80}-$TFBM_{20}$. At FBM_{90}-$TFBM_{10}$ the precision slightly decreased to 89%, which can be explained by the incomplete *para* fluorine conversion of 93%. Nevertheless, the power of mixed flow-PFTR to precisely modify poly(PFSty) towards desired chemical compositions with mixtures of thiols by virtue of flow chemistry could be confirmed (refer to Fig. 6D). SEC analysis of poly(PFSty-FBM-*r*-TFBM) revealed an increase in M_n from 19 000 g mol^{-1} to 25 200–23 400 g mol^{-1}. Interestingly, the M_n of poly(PFSty-FBM-*r*-TFBM) increased linearly with incorporation of heavier TFBM moieties in the polymer while $Đ$ remained constant overall at approximately 1.23 (refer to Fig. 7A and SI, Fig. S25). In comparison to DT-containing polymers presented in this study, the thermal decomposition of poly(PFSty-FBM-*r*-TFBM) was largely unaffected by the ratio of modification and both $T_{5\%}$ and the residual weight at 800 °C remained constant with 321 °C and 33 wt%, respectively (refer to Fig. 7B and SI, Table S7). The T_g of poly(PFSty-FBM-*r*-TFBM) was found to be in the range of 48–58 °C and notably depended linearly on the ratio of modification between FBM and TFBM (refer to Fig. 7C and SI, Fig. S26).

All in all, these results demonstrate the beneficial applicability of mixed flow-PFTR to create polymer materials with desired macroscopic properties directly by controlling the feed ratio of reactants.

Conclusions

We reported the polymerisation and PPM of PFSty in continuous flow. The RAFT polymerisation of PFSty was systematically investigated at different temperatures (70–100 °C) and with varying RAFT agents (CPDT, CDCTPA, DoPAT, and CBCDMPC). Monomer conversion and molecular weight analysis were automatically measured by an autonomous flow reactor platform able to perform kinetic analysis by transient timesweeping. The polymerisation was well-controlled up to 90 °C before exceeding the feasible AIBN operation temperature. Apparent polymerisation rate coefficients ranged from 1.18×10^{-3} to 1.13×10^{-2} s^{-1} at 70–90 °C. The kinetic behaviour of the PPM of poly(PFSty) by PFTR in continuous flow was conducted with three different thiols (DT, FBM, and TFBM) at 50, 60, and 70 °C. FBM was found to quantitatively undergo PFTR within 5 minutes at all temperatures while TFBM was found to react slower with full conversion after 6 minutes at 60 and 70 °C and 12 minutes at 50 °C. The PFTR of poly(PFSty) with DT was found to be complete after 1 minute for all temperatures, however, the conversion did not exceed 53% at 70 °C, likely due to steric hindrance. A dedicated structure analysis regarding the substitution pattern of poly(PFSty) by DT and other thiols was beyond the scope of this work but might be a prom-

ising study for future research on the structural control of polymers modified *via* PFTR. Additionally, the control over polymer modification by mixed flow-PFTR was demonstrated using an adapted flow platform capable to carry out 4-component reactions. Poly(PFSty) was modified with 88–99% precision using mixtures of DT-FBM while mixtures of DT-TFBM allowed for modification with 82–97%. It can be concluded that similar reactivities in both modifying agents for the PFTR are favourable for precise control over the polymer modification. While the PFTR was generally fast for all investigated thiols, steric hindrance and selective reactivities were found to be a decisive factor to ensure stochiometric incorporation of substituents into the resulting polymer and therefore enable direct polymer prediction based on input feed ratios. This was showcased by the mixed flow-PFTR with FBM-TFBM, showing a precision of over 95% for most input feed ratios. Additional SEC, TGA, and DSC analysis highlighted the versatility of poly(PFSty) as platform and adaptable polymer material with controllable structures and properties at low $Đ$. We believe that the approach described herein is well suited for small-scale optimization, enabling efficient transfer of optimized conditions to larger-scale synthesis. Potential reactor scale-up will mainly be constrained by mixing and heat transfer, requiring enhanced mixing strategies and precise temperature control to ensure reproducible product quality. While this work focused only on the investigation of poly(PFSty) homopolymers, development of more complex structures and architectures by exploitation of orthogonal reactions becomes very feasible with the presented method. The usage of predictive flow-polymer chemistry based on ML with functional monomers such as PFSty for kinetic modelling and transfer to batch presents itself as a promising future route to obtain tailor-made polymers.[69] Additionally, realisation of a telescoped reaction which includes polymerisation and PPM of PFSty or other functional monomers in one stream is believed to be an exciting approach to further develop the method presented herein. We are convinced that the strategy described herein is an important step to unlock rapid material discovery utilising flow-PFTR by the means of automated flow polymer chemistry.

Author contributions

A. P. G.: conceptualisation, data curation, investigation, methodology, formal analysis, visualisation, writing – original draft, writing – review & editing; A. B. A.: data curation, methodology, software, writing – original draft, writing – review & editing; B. S.: formal analysis, visualisation, writing – original draft, writing – review & editing; C. W. S.: project administration, supervision, writing – review & editing; D. V.: project administration, supervision, writing – review & editing; T. J.: conceptualisation, funding acquisition, methodology, project administration, supervision, writing – review & editing; P. T.: funding acquisition, project administration, supervision, writing – review & editing.

Conflicts of interest

There are no conflicts to declare.

Data availability

Raw data sets can be found in the RADAR4Chem repository under the following digital object identifier: https://doi.org/10.22000/mepywt3798mzqdzr.

Supplementary information (SI): raw data sets. See DOI: https://doi.org/10.1039/d5py01142f.

Acknowledgements

A. P. G., B. S., C. W. S., and P. T. acknowledge funding from the Helmholtz Association. A. P. G. thanks the Karlsruhe House of Young Scientists for financial support *via* the Research Travel Grant. A. B. A. and T. J. are grateful for funding from Monash University and the Australian Research Council *via* project DP240100120.

References

1 Y. Shen, J. E. Borowski, M. A. Hardy, R. Sarpong, A. G. Doyle and T. Cernak, *Nat. Rev. Methods Primers*, 2021, **1**, 23.
2 K. G. Reyes and B. Maruyama, *MRS Bull.*, 2019, **44**, 530–537.
3 I. W. Davies, *Nature*, 2019, **570**, 175–181.
4 C. W. Coley, D. A. Thomas, J. A. M. Lummiss, J. N. Jaworski, C. P. Breen, V. Schultz, T. Hart, J. S. Fishman, L. Rogers, H. Gao, R. W. Hicklin, P. P. Plehiers, J. Byington, J. S. Piotti, W. H. Green, A. J. Hart, T. F. Jamison and K. F. Jensen, *Science*, 2020, **365**, 6453.
5 D. Paul, G. Sanap, S. Shenoy, D. Kalyane, K. Kalia and R. K. Tekade, *Drug Discovery Today*, 2021, **26**, 80–93.
6 R. F. Service, *Science*, 2023, **382**, 987.
7 L. Zhichao, M. Dong, L. Xiongjun and Z. Lu, *Commun. Mater.*, 2024, **5**, 76.
8 D. Kuntz and A. K. Wilson, *Pure Appl. Chem.*, 2022, **94**, 1019–1054.
9 R. Geyer, in *Plastic Waste and Recycling*, ed. T. M. Letcher, Academic Press, 2020, pp. 13–32.
10 B. A. Abel and G. W. Coates, *Chem. Rev.*, 2025, **125**, 1255–1256.
11 M. Hempel, *Chem. Eng. Technol.*, 2009, **32**, 1651–1654.
12 V. Hessel, D. Kralisch, N. Kockmann, T. Noël and Q. Wang, *ChemSusChem*, 2013, **6**, 746–789.
13 R. L. Hartman, J. P. McMullen and K. F. Jensen, *Angew. Chem., Int. Ed.*, 2011, **50**, 7502–7519.
14 N. Zaquen, M. Rubens, N. Corrigan, J. Xu, P. B. Zetterlund, C. Boyer and T. Junkers, *Prog. Polym. Sci.*, 2020, **107**, 101256.

15 N. Kockmann, P. Thenée, C. Fleischer-Trebes, G. Laudadio and T. Noël, *React. Chem. Eng.*, 2017, **2**, 258–280.
16 J. Wang, L. Ni, J. Cui, J. Jiang and K. Zhou, *Processes*, 2020, **8**, 1650.
17 P. R. Judzewitsch, N. Corrigan, F. Trujillo, J. Xu, G. Moad, C. J. Hawker, E. H. H. Wong and C. Boyer, *Macromolecules*, 2020, **53**, 631–639.
18 O. Weismantel, L. J. Weerarathna and T. Junkers, *ACS Appl. Polym. Mater.*, 2025, **7**, 938–947.
19 M. Rubens, J. H. Vrijsen, J. Laun and T. Junkers, *Angew. Chem., Int. Ed.*, 2019, **58**, 3183–3187.
20 L. Vaccaro, D. Lanari, A. Marrocchi and G. Strappaveccia, *Green Chem.*, 2014, **16**, 3680–3704.
21 V. W. K. R. Barnikol and G. V. Schulz, *Die Makromol. Chem.*, 1963, **68**, 211–215.
22 D. N. Bhattacharyya, C. L. Lee, J. Smid and M. Szwarc, *J. Am. Chem. Soc.*, 1963, **85**, 533–539.
23 C. Geacintov, J. Smid and M. Szwarc, *J. Am. Chem. Soc.*, 1962, **84**, 2508–2514.
24 V. H. Hostalka, R. V. Figini and G. V. Schulz, *Die Makromol. Chem.*, 1964, **71**, 198–203.
25 M. H. Reis, F. A. Leibfarth and L. M. Pitet, *ACS Macro Lett.*, 2020, **9**, 123–133.
26 T. Junkers, J. P. Hooker, J. van Herck, A. Kumar and G. D. Ammini, *Polym. Chem.*, 2023, **14**, 2708–2716.
27 A. Sivokhin, D. Orekhov, O. Kazantsev, K. Otopkova, O. Sivokhina, Y. Chesnokov, M. Smirnov, A. Ovchinnikov and I. Makhov, *Polym. Chem.*, 2023, **14**, 3186–3195.
28 M. A. Beres, B. Zhang, T. Junkers and S. Perrier, *Polym. Chem.*, 2024, **15**, 3166–3175.
29 S. Zhang, T. Junkers and S. Kuhn, *Chem. Sci.*, 2022, **13**, 12326–12331.
30 A. K. Padmakumar, N. K. Singha, M. Ashokkumar, F. A. Leibfarth and G. G. Qiao, *Macromolecules*, 2023, **56**(17), 6920–6927.
31 A. A. Cockram, R. D. Bradley, S. A. Lynch, P. C. D. Fleming, N. S. J. Williams, M. W. Murray, S. N. Emmett and S. P. Armes, *React. Chem. Eng.*, 2018, **3**, 645–657.
32 J. D. Guild, S. T. Knox, S. B. Burholt, E. M. Hilton, N. J. Terrill, S. L. M. Schroeder and N. J. Warren, *Macromolecules*, 2023, **56**, 6426–6435.
33 P. M. Pittaway, K. E. Chingono, S. T. Knox, E. Martin, R. A. Bourne, O. J. Cayre, N. Kapur, J. Booth, R. Capomaccio, N. Pedge and N. J. Warren, *ACS Polym. Au*, 2025, **5**, 1–9.
34 K. S. C. Jäger, G. D. Ammini, P.-J. Voorter, P. Subramanian, A. Kumar, A. Anastasaki and T. Junkers, *J. Am. Chem. Soc.*, 2025, **147**, 594–602.
35 L. Goehringer, G. D. Ammini and T. Junkers, *Faraday Discuss.*, 2026, **262**, 500–514.
36 S. Mozharov, A. Nordon, D. Littlejohn, C. Wiles, P. Watts, P. Dallin and J. M. Girkin, *J. Am. Chem. Soc.*, 2011, **133**, 3601–3608.
37 J. S. Moore and K. F. Jensen, *Angew. Chem., Int. Ed.*, 2014, **53**, 470–473.
38 J. J. Haven, N. Zaquen, M. Rubens and T. Junkers, *Macromol. React. Eng.*, 2017, **11**, 1700016.
39 J. van Herck and T. Junkers, *Chem.:Methods*, 2022, **2**, e202100090.
40 A. D. Clayton, A. M. Schweidtmann, G. Clemens, J. A. Manson, C. J. Taylor, C. G. Niño, T. W. Chamberlain, N. Kapur, A. J. Blacker, A. A. Lapkin and R. A. Bourne, *Chem. Eng. J.*, 2020, **384**, 123340.
41 S. T. Knox, S. J. Parkinson, C. Y. P. Wilding, R. A. Bourne and N. J. Warren, *Polym. Chem.*, 2022, **13**, 1576–1585.
42 S. T. Knox, K. E. Wu, N. Islam, R. O'Connell, P. M. Pittaway, K. E. Chingono, J. Oyekan, G. Panoutsos, T. W. Chamberlain, R. A. Bourne and N. J. Warren, *Polym. Chem.*, 2025, **16**, 1355–1364.
43 M. Rubens, J. van Herck and T. Junkers, *ACS Macro Lett.*, 2019, **8**, 1437–1441.
44 J. van Herck, I. Abeysekera, A.-L. Buckinx, K. Cai, J. Hooker, K. Thakur, E. van de Reydt, P.-J. Voorter, D. Wyers and T. Junkers, *Digital Discovery*, 2022, **1**, 519–526.
45 T. Nwoko, B. Zhang, T. Vargo, T. Junkers and D. Konkolewicz, *Macromolecules*, 2025, **58**, 488–494.
46 L. Dumas, E. Fleury and D. Portinha, *Polymer*, 2014, **55**, 2628–2634.
47 L. M. Han, R. B. Timmons, W. W. Lee, Y. Chen and Z. Hu, *J. Appl. Phys.*, 1998, **84**, 439–444.
48 C. R. Becer, K. Babiuch, D. Pilz, S. Hornig, T. Heinze, M. Gottschaldt and U. S. Schubert, *Macromolecules*, 2009, **42**, 2387–2394.
49 S. Chen, A. Funtan, F. Gao, B. Cui, A. Meister, S. S. P. Parkin and W. H. Binder, *Macromolecules*, 2018, **51**, 8620–8628.
50 G. Delaittre and L. Barner, *Polym. Chem.*, 2018, **9**, 2679–2684.
51 A. P. Grimm, S. T. Knox, C. Y. P. Wilding, H. A. Jones, B. Schmidt, O. Piskljonow, D. Voll, C. W. Schmitt, N. J. Warren and P. Théato, *Macromol. Rapid Commun.*, 2025, e2500264.
52 C. J. Ferguson, R. J. Hughes, D. Nguyen, B. T. T. Pham, R. G. Gilbert, A. K. Serelis, C. H. Such and B. S. Hawkett, *Macromolecules*, 2005, **38**, 2191–2204.
53 L. K. Kostanski, D. M. Keller and A. E. Hamielec, *J. Biochem. Biophys. Methods*, 2004, **58**, 159–186.
54 A. B. Asghar, B. Zhang, V. F. Jafari and T. Junkers, *React. Chem. Eng.*, 2026, **11**, 160–169.
55 A. Theis, A. Feldermann, N. Charton, M. H. Stenzel, T. P. Davis and C. Barner-Kowollik, *Macromolecules*, 2005, **38**, 2595–2605.
56 C. Barner-Kowollik, *Handbook of RAFT polymerization*, Wiley-VCH, Weinheim, 2008.
57 M. Teodorescu and K. Matyjaszewski, *Macromol. Rapid Commun.*, 2000, **21**, 190–194.
58 H. Zhang, Y. Wang, J. Yang, Y. Ju, J. He, Y. Niu, Y. Liu, W. Hou, L. Qiao and J. Jiang, *Chem. – Eur. J.*, 2025, **31**, e202404036.
59 M. Chen, G. Moad and E. Rizzardo, *J. Polym. Sci., Part A: Polym. Chem.*, 2009, **47**, 6704–6714.
60 T. Zhao, V. P. Beyer and C. R. Becer, *Macromol. Rapid Commun.*, 2020, **41**, 2000409.

61 *Functional polymers by post-polymerization modification: Concepts, guidelines, and applications*, ed. H.-A. Klok and P. Theato, Wiley-VCH, Weinheim, 2013.
62 J. Clayden, N. Greeves and S. G. Warren, *Organic chemistry*, Oxford University Press, Oxford; New York; Auckland, 2nd edn, 2012.
63 C. M. Brown, K. E. L. Husted, Y. Wang, L. J. Kilgallon, P. Shieh, H. Zafar, D. J. Lundberg and J. A. Johnson, *Chem. Sci.*, 2023, **14**, 8869–8877.
64 N. A. Belov, D. S. Pashkevich, A. Y. Alentiev and A. Tressaud, *Membranes*, 2021, **11**, 713.
65 B. Hendriks, J. Waelkens, J. M. Winne and F. E. Du Prez, *ACS Macro Lett.*, 2017, **6**, 930–934.
66 V. Scholiers, S. M. Fischer, B. Daelman, S. Lehner, S. Gaan, J. M. Winne and F. E. Du Prez, *Angew. Chem., Int. Ed.*, 2025, **64**, e202420657.
67 S. A. Tharakan and S. Muthusamy, *RSC Adv.*, 2021, **11**, 16645–16660.
68 P. Zhu, W. Meng and Y. Huang, *RSC Adv.*, 2017, **7**, 3179–3189.
69 J. D. Tan, B. Ramalingam, S. L. Wong, J. J. W. Cheng, Y.-F. Lim, V. Chellappan, S. A. Khan, J. Kumar and K. Hippalgaonkar, *J. Chem. Inf. Model.*, 2023, **63**, 4560–4573.